Quantifying the dynamics of viral recombination during free virus and cell-to-cell transmission in HIV-1 infection

Jesse Kreger[1], Josephine Garcia[2], Natalia L. Komarova[1], Dominik Wodarz[3,1], and David N. Levy[2]

1: Department of Mathematics, Rowland Hall, University of California, Irvine CA 92697

2: Department of Basic Science, New York University College of Dentistry, 921 Schwartz Building, 345 East 24th Street, New York, NY 10010 – 9403, USA

3: Department of Population Health and Disease Prevention, Program in Public Health, Susan and Henry Samueli College of Health Sciences, University of California, Irvine, CA 92697

Abstract

Recombination has been shown to contribute to HIV-1 evolution *in vivo*, but the underlying dynamics are extremely complex, depending on the nature of the fitness landscapes and of epistatic interactions. A less well-studied determinant of recombinant evolution is the mode of virus transmission in the cell population. HIV-1 can spread by free virus transmission, resulting largely in singly infected cells, and also by direct cell-to-cell transmission, resulting in the simultaneous infection of cells with multiple viruses. We investigate the contribution of these two transmission pathways to recombinant evolution, by applying mathematical models to *in vitro* experimental data on the growth of fluorescent reporter viruses under static conditions (where both transmission pathways operate), and under gentle shaking conditions, where cell-to-cell transmission is largely inhibited. The parameterized mathematical models are then used to extrapolate the viral evolutionary dynamics beyond the experimental settings. We find that recombinant evolution is fastest if only synaptic transmission operates, and that the addition of free virus transmission reduces the number of recombinants at a given infected cell population size. This is due to synaptic transmission (i) increasing infection multiplicity, (ii) promoting the co-transmission of different virus strains from cell to cell, and (iii) increasing the rate at which point mutations are generated as a result of more reverse transcription events. This work further resulted in the estimation of various parameters that characterize these evolutionary processes. For example, we estimate that during cell-to-cell transmission, an average of 3 viruses successfully integrated into the target cell, which can significantly raise the infection multiplicity compared to free virus transmission. In general, our study points towards the importance of infection multiplicity and cell-to-cell transmission for HIV-evolution within patients.

Introduction

Human immunodeficiency virus-1 (HIV-1) infection eventually results in the development of AIDS, typically after several years. Viral evolution is thought to be a major contributor to disease progression, and poses important challenges to antiviral treatments and to the development of protective vaccines [1-3]. HIV-1 is characterized by a relatively high mutation rate ($3x10^{-5}$ per base pair per generation) [4], which, together with the fast turnover of the virus population [5-7] contributes to the large evolutionary potential of the virus. Besides mutations, however, HIV-1 can also undergo recombination because the virions are diploid [8, 9]. If a cell is infected with two different virus strains and two different genomes are packaged into the offspring virus, recombination can occur between these two strains when the virus infects a new cell and undergoes reverse transcription. Recombination can accelerate the generation of 2-hit mutant viruses from two different 1-hit mutants, which is likely faster than the generation of 2-hit mutants by point mutations alone. These processes can be especially relevant for the evolution of viral variants that simultaneously escape multiple immune cell clones or drugs.

While recombination has been shown to significantly contribute to viral evolution in vivo [9], mathematical models have demonstrated that the dynamics of recombination can be extremely complex [10-15]. Recombination can not only help the generation of multi-hit mutants, it can also break existing mutant combinations apart. The net effect of recombination is difficult to predict and depends on underlying assumptions about fitness landscapes, the nature and magnitude of epistatic interactions, and the relative

balance of free virus and direct cell-to-cell transmission. Efforts have been made to quantify some of those processes, such as the fitness landscapes and the nature of epistasis in the evolution of drug resistance [16].

Here, we seek to quantify in detail how the different virus transmission pathways impact the evolution of recombinants. The nature of virus transmission during viral spread through the cell population is likely crucial for the rate of recombinant evolution, through variations in infection multiplicity [17-19]. Free virus transmission typically results in the infection of cells containing one virus, while direct cell-to-cell transmission through virological synapses typically results in the multiple infection of cells, and additionally is likely to result in the co-transmission of different virus strains from one cell to the next [18, 19]. Therefore, cell-to-cell (or synaptic) transmission is likely to be beneficial for the rate at which viral recombinants emerge.

Here, we combine mathematical models with *in vitro* experiments that utilize fluorescent reporter viruses [8] to test this hypothesis, to quantify the dynamical processes that lead to recombinant generation, and to estimate underlying parameters. Viruses can carry genes for cyan fluorescent protein (eCFP) and yellow fluorescent protein (eYFP). Recombination between these two variants results in viruses characterized by green fluorescence in target cells [8]. Additionally, recombination of the green fluorescent virus with a non-glowing virus can break the recombinant apart, resulting in yellow and cyan fluorescent viruses. The viral transmission pathway can be modulated by placing the culture on a gentle rocking platform [20, 21], which disrupts

synaptic transmission. The frequency of infected cells displaying cyan, yellow and/or green is measured by flow cytometry over several days after infection. Mathematical models are applied to these experimental data to quantitatively characterize the dynamics.

Materials and Methods

Experimental setup

2 x10^6 CEM-SS cells were infected with 25μL NLENY1-IRES (YFP) or NLENC1-IRES (CFP), representing 19 virions/cell, by spinoculation at 1200g for 2 hours at 37°C as described previously [22]. Cells were cultured in Gibco Advanced RPMI-1640 with 5% FBS plus penicillin and streptomycin and 50 μM β-mercaptoethanol. The next day these cells were washed and YFP and CFP infected cells were mixed with uninfected CEM-SS cells.

Three independent experiments were performed at the following cell numbers in 3 ml of culture medium in T-75 flasks:

Expt	Subset	YFP+CFP x 10^6	Uninfected x 10^6
1, 2, 3	A	0.75	2
1, 2, 3	B	0.3	2
1, 2	C	0.075	2

These cultures were established in duplicate, one for the stationary condition and one for the rocking condition. The stationary set of cultures was placed on a shelf of a TC

incubator at a 10° angle to concentrate the cells at one end. The rocking set was placed on a rocking platform in the incubator set at 12 tilts per minute. On each subsequent day 1/8-1/4 of the culture was collected for flow cytometry for YFP, CFP and GFP as previously described [8]. New culture medium was added to maintain a consistent volume in each culture.

Mathematical models

We consider an ordinary differential equation (ODE) model of virus dynamics that tracks the populations of uninfected cells, as well as different types of infected cell populations. Due to the complexity of the equations, they are displayed in the Supplementary Materials, and basic assumptions are outlined here. Cells can be infected with (i) single-mutant viruses that carry cyan fluorescent protein, C, and yellow fluorescent protein, Y; (ii) the recombinant virus strain that shows green fluorescence (G); and (iii) the non-glowing virus strain that does not show any fluorescence, W. Hence, the model tracks cell populations that are infected with any combination of these virus strains, at defined multiplicities (i.e. cells can contain *i* copies of C, *j* copies of Y, *k* copies of G, and *l* copies of W viruses). The fitness of all virus types is assumed to be identical.

The uninfected cell population is assumed to divide with a doubling time of 18 hours. The infection is assumed to be transmitted by two different pathways: (i) free virus transmission, where one copy of virus is transferred to the target cell, and (ii) direct cell-to-cell transmission through virological synapses, where S viruses are simultaneously transferred to the target cell. These infection processes are assumed to

be non-spatial. During the infection process, the model assumes that recombination can occur with a certain probability if the infecting virus carries two genetically different genomes. All possible recombination events are described in the Supplementary Materials.

Three versions of this model with rising biological complexity are considered. (i) The basic form of the model contains the assumptions outlined above. (ii) A more complex form of the model assumes that upon virus integration into an uninfected cell, there is a certain probability that the virus will become latent and not display fluorescence. Moreover, it is assumed that superinfection of such a cell with another virus can activate the latent virus in this cell, which can thus result in fluorescence [23]. (iii) In a further layer of complexity, we assume a modification to the perfect mixing assumption of the basic model. In particular, we explore the possibility that viruses released from an infected cell can re-enter the same cell and generate a recombinant virus in this cell, resulting in a different distribution of cells that are multiply infected with different virus strains including the recombinant.

The different models are fit to the experimental data with standard methods, and the model that is most powerful at explaining the data is selected with the F-test for nested models. Details of all these models are again given in the Supplementary Materials.

Results

Basic dynamics

The experimental system and the mathematical models are described in Materials and Methods, with additional details given in the Supplementary Materials. Based on previous work by others and us [20, 21], In vitro virus growth experiments were performed under two conditions: (i) under static conditions in which both free virus and synaptic transmission operate, and (ii) under shaking conditions where cultures were placed on a gentle rocking platform, which prevents most synaptic transmission events from taking place. For each transmission pathway, eight experiments were performed that differed in viral inoculum size. Time-series were obtained for each condition, where we tracked cells infected with two types of single-hit mutant: those labeled with cyan fluorescent protein, denoted as C, and those labeled with yellow fluorescent protein, denoted as Y. In addition, we followed the population of cells infected with double-hit mutants labeled with green fluorescent protein, denoted as G, as well as populations of cells that contained combinations of virus types, such as YC, YG, CG, and YCG. Examples of this can be seen in Figures 1 (shaking condition) and 2 (static condition).

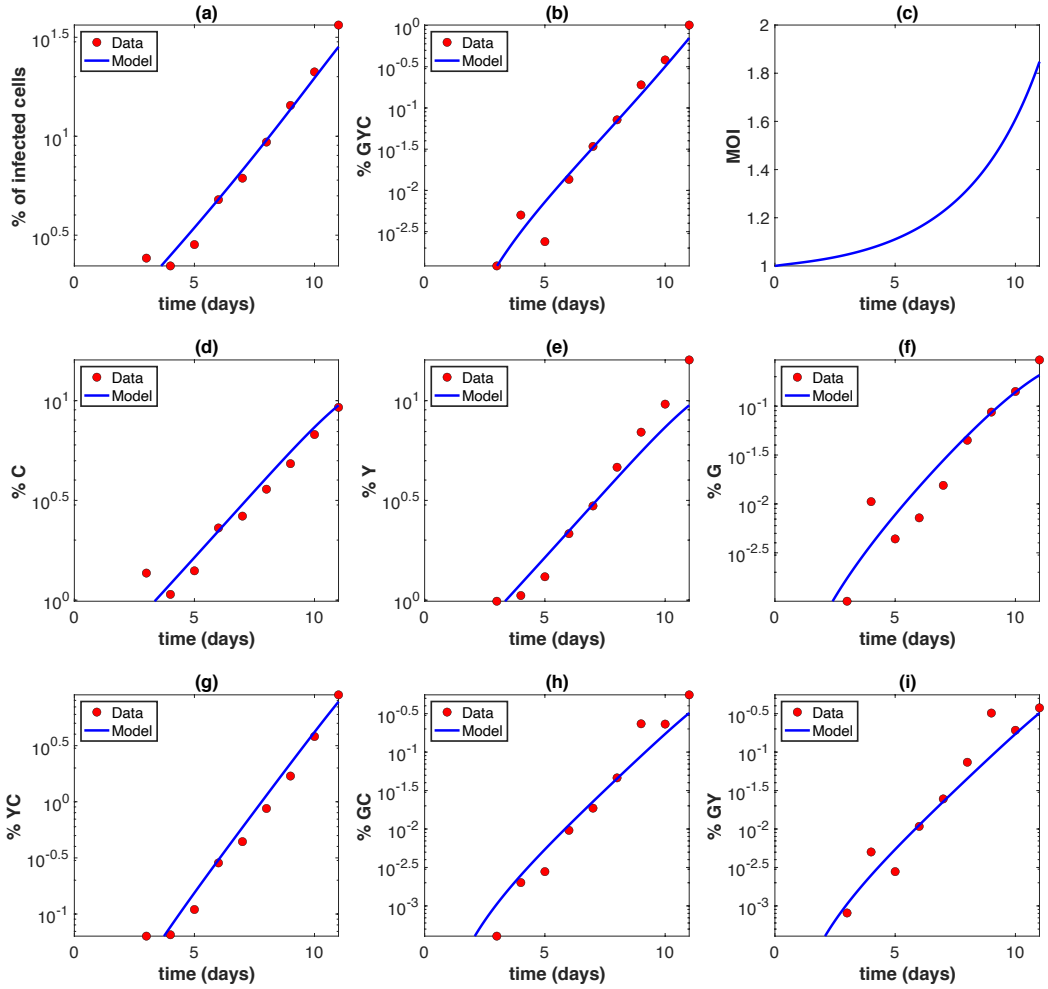

Figure 1: Example of a shaking experiment (experiment A6). The experimental data (red circles) is presented with best fit curves from the model (blue lines). The mathematical model is described in the Materials and Methods section with details in the Supplementary Materials, and the fitting procedure is described in the Supplementary Materials. Best fit parameters are included in Table 2 in the Supplementary Materials. The horizontal axis for all panels represents time (days). (a) The overall percentage of infected cells. (b) The percentage of cells infected with at least one copy of G, Y, and C. (c) The average multiplicity of infection (MOI) over all infected cells. (d) The percentage of cells infected with at least one active copy of C. (d) The percentage of cells infected with at least one active copy of Y. (f) The percentage of cells infected with at least one active copy of G. (g) The percentage of cells infected with at least one copy of Y and C. (h) The percentage of cells infected with at least one copy of G and C. (i) The percentage of cells infected with at least one copy of G and Y.

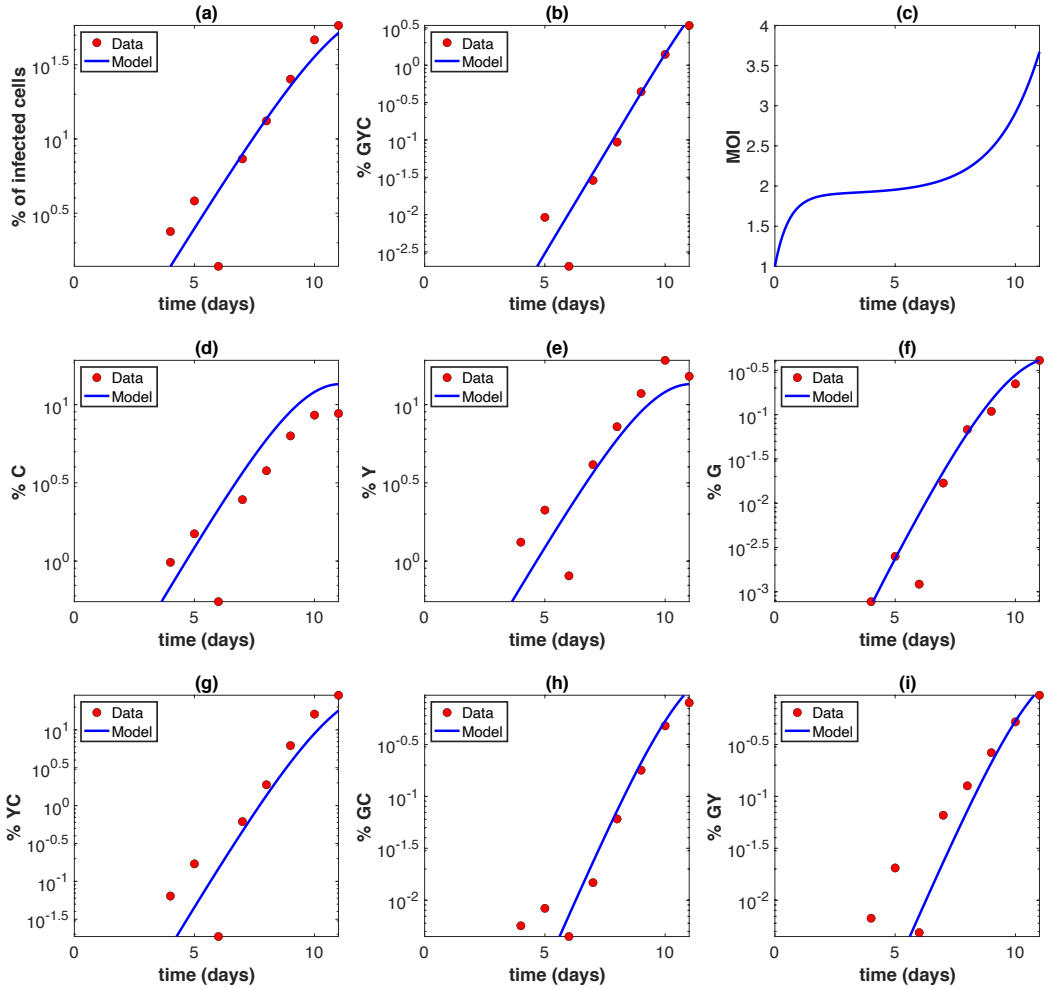

Figure 2: Example of a static, non-shaking experiment (experiment B2). Everything is the same as in Figure 1, except best fit parameters are included in Table 3 in the Supplementary Materials.

As expected, exponential growth was observed for the total population of infected cells. This growth was faster under static compared to shaking conditions, resulting in higher virus levels for static conditions during the time frame of the experiment (Figure 2). Applying basic virus dynamics models to data that describe the growth of the total virus population allowed us to estimate the growth rate of the virus in the shaking and static conditions, and hence to estimate the rate of free virus transmission and the rate of synaptic transmission. Previous work showed that shaking can increase the rate of

free virus spread compared to static cultures due to mixing the virus more efficiently among the cells, by a factor of approximately f=1.33 [21]. Therefore, we corrected for this when calculating the rate of free virus spread from the shaking experiments (full details of the methodology is given in Materials and Methods). According to our calculations, the rate of free virus spread was on average 1.44±0.13 fold higher than the rate of synaptic transmission. In our previous study, these rates were more equal, with the rate of free virus transmission being on average 1.1±0.1 fold higher than the rate of synaptic transmission. The difference is likely due to the different T cell lines used in the experiments (Jurkat cells in the previous study vs CEM-ss cells in the current one), and due to the fact that we did not take into account the possibility of latent infection in our previous study, which increases the estimated rate of free virus transmission.

Multiple infection dynamics

Next, we examined the ability of the mathematical model to predict the dynamics of double color cells, i.e. cells containing both Y and C reporter viruses. Consistent with previous work [23], the model in its most basic forms failed to accurately predict the number of YC infected cells over time. The basic model appears to under-predict the cell numbers, and we hypothesized that this happens because of latent infection and virus activation following superinfection. It has been demonstrated that infection can result in the generation of a latently infected cell, but that super-infection can result in the activation of the latent virus. The reason is that superinfection results in TAT complementation and thus activation of the latent genome in the cell [23]. For example, if a virus becomes infected with Y virus, it can become latent and the infected cell will

not glow. Subsequent superinfection with C virus, however, will result in an infected cell that glows in both colors. As a consequence, the observed (glowing) population of singly infected cells is smaller than the actual population, which can explain why the observed number of YC cells are consistently larger than the predicted ones. Hence, we expanded the model to assume that upon single infection, the virus goes latent with a probability ε, and that subsequent superinfection activates this virus. Such a model can now predict the YC population more accurately, as determined statistically by the F-test for nested models (Figure S2). The probability for the virus to become latent upon single infection was rather consistent across the different experiments, with an average of $\varepsilon=0.24\pm 0.075$. In other words, about a quarter of all infection events of uninfected cells are estimated to result in viral latency in this system.

Multiple infection and recombinant dynamics under shaking conditions

Next, we determined how well the model that we parameterized thus far can predict the observed number of cells that carry the recombinant virus (green). We found that the model consistently underpredicted multiply infected cells that contained the recombinant virus, i.e. the triple color YCG cells and double color cells YG and CG, although the number of cells infected with only double-hit mutants (G) cells could be predicted more accurately (Figure S3). We hypothesized that although shaking results in the mixing of cells, the perfect mixing dynamics assumed by our ordinary differential equation model might be responsible for this discrepancy.

In particular, we propose that when e.g. a YC-infected cells releases virus particles, they are likely to re-enter the same cell and generate a G virus upon recombination, thus explaining the higher than expected number of YCG cells. The reason is that as viruses are released from a cell, this cell is unlikely to immediately move away from its present location, but rather remains in the current vicinity for a while, which makes re-infection a likely event. Similarly, if a cell is infected with GW (where “W” stands for non-glowing virus) and only glows green, recombination between G and W can give rise to a C or a Y virus. Re-infection of the same cell with these viruses can then yield GCW and GYW cells (which glow in two colors). We first tested this idea with an agent-based model (ABM) that tracked the spatial location of cells and included diffusion of virus and movement of cells to simulate a more limited degree of mixing. Preliminary explorations indicated that such a model could account for the data more accurately, but due to the complexity of the model and the corresponding data fitting procedures, we decided not to proceed with the ABM. Instead, we modified the ODE model to capture the assumption about a higher frequency of self-infection phenomenologically (see Supplementary Materials). This model, while still compatible with a straightforward fitting procedure, could more accurately describe the GYC, GY, and GC data than the previous models (Figure S3), and was determined to be a more powerful model (despite containing an extra “self-infection” parameter) by the F-test for nested models. These results indicate that the straightforward perfect mixing ODE models that are typically used to describe virus dynamics are not accurate descriptions of the dynamics at the level of detail presented here.

With this model we estimated the recombination rate to be $\rho = 0.355 \pm 0.066$. This is close to the maximally possible recombination rate of $\rho = 0.5$ in this model (see Supplementary Materials). The model also allowed us to estimate the average multiplicity of infection within the cells in the different experiments under the shaking conditions (Figure 1). As expected, multiplicity increased as the viral population grew to higher levels, with multiplicities ranging between 1 and 1.8 during the time frame of the experiments (Figure 1(c)).

Recombinant dynamics under static conditions

To fit the static data (Figure 2), we took the parameter estimates from the corresponding shaking experiment and fitted the full model, thus measuring additional parameters associated with synaptic transmission. The rate of synaptic transmission was estimated with the simpler version of the model above (without multiplicity and recombination), and here we discuss parameters connected to multiple infection. An important question concerns the number of viruses that are transferred from one cell to another through virological synapses during cell-to-cell transmission. Experimental data indicate that virus transfer through virological synapses is a very efficient process, with tens to hundreds of viruses transferred [17, 24]. Not all of these viruses, however, are likely to successfully integrate into the genome of the target cell. In our experiments, we estimated that on average $s=3.0 \pm 0.53$ viruses successfully infect a target cell per synaptic transmission event. The average infection multiplicity ranged from 1-8 during the time frame of the static experiments (compared with a much lower estimate of maximum 1.8 under shaking conditions, see Figure 2(c)).

Comparing the effect of viral transmission pathways on recombinant generation: beyond the experimental setup

The experimental setup discussed above represents an artificial system to parameterize an evolutionary model of viral recombination. Here we use the parameterized model to simulate the dynamics in more general terms and to go beyond the experimental setup in the following ways.

(i) Shaking conditions resulted in largely free virus transmission, while static conditions allowed both free virus and synaptic transmission to proceed. Using the estimated parameters in computer simulations, we further predict the dynamics for a scenario where only synaptic transmission takes place, which was not feasible experimentally.

(ii) Due to the inherent differences in viral growth rates in the shaking and static experiments, the number of infected cells to which the infection grew was significantly smaller for the shaking experiments during the time frame of the experiment. This makes a comparison of recombinant evolution difficult. Using the estimated parameters, we can simulate growth of the virus population to the same population size *in silico* and compare the number of recombinants that have been generated for the different assumed transmission pathways. Along similar lines, we can adjust the infection rates such that the overall rate of virus growth is the same independent of which transmission pathways are at work.

(iii) The experimental system is an artificially constructed system that was used to measure key parameters connected to recombinant evolution. We can use the parameterized equations to move beyond this artificial system and describe a more complete evolutionary picture. That is, we can start with a "wild-type" virus (which was not part of the experimental setup) and model the generation of single-hit mutants by point mutation (which would technically correspond to the Y and C viruses, even though these reporter viruses are not generated by single mutation events in the experiments), and the subsequent evolution of double mutants through recombination (which would correspond to G viruses).

First, we considered simulations that start with an equal number of single-mutant viruses and ignore point mutations for now. We started the simulations with 10^9 uninfected cells, and in contrast to the experiments, we did not allow for exponential expansion of the uninfected cell population, because lack of extensive cell growth corresponds better to the conditions in which virus grows during acute HIV infection *in vivo*. We let the total number of infected cells grow until a population size of $4x10^8$ cells was reached. This was done assuming that only free virus transmission, only synaptic transmission, or both types of transmission occur. The number of cells that contain the recombinant virus was quantified as a function of time and total infected cell population size (Figure 3(a and b)). If we consider the number of recombinants that appear over time in the simulations, recombinants rise the fastest if both transmission pathways operate, compared to only a single active transmission pathway. This is due to the fact

that synaptic transmission promotes recombinant generation through repeated co-transmission of single-mutant viruses, but also due to both transmission types resulting in the fastest overall rate of viral growth. To compare the effect of the transmission pathways themselves on recombinant generation (independent of the differences in viral growth rates), we determined the number of recombinants as a function of the total infected cell population size (rather than time) (Figure 3(b)). We observe that synaptic transmission alone yields the largest number of recombinants, followed by the simulation with both transmission pathways. Free virus transmission alone results in the lowest number of recombinants. The reason for these observations is that synaptic transmission increases the chances for recombination to occur through the repeated co-transmission of single-mutant viruses. If both synaptic and free virus transmission operate, the same total infected cell population size is reached with fewer synaptic transmission events (due to the existence of free virus transmission), thus resulting in a lower number of recombinants. Infection multiplicity is also key in these dynamics (Figure 3a inset)). Synaptic transmission results in the highest number of viruses per infected cell, which facilitates both co-transmission of different viral strains and recombination.

As an alternative way to correct for the differences in viral growth rates associated with the different transmission pathways, we further assumed that the overall growth rate (or doubling time) of the virus was identical for all transmission pathways (and identical to that observed in the static experiments) (Figure 3c and d). We again observe that recombinant cells rise fastest if the virus only spreads through synaptic

transmission. A combination of both transmission pathways again results in a slower rate of recombinant emergence, and recombinants evolve slowest if only free virus transmission occurs.

Next, we consider a more complete evolutionary scenario. We start with a wild-type virus only, and introduce point mutations into the model. The wild-type virus can thus

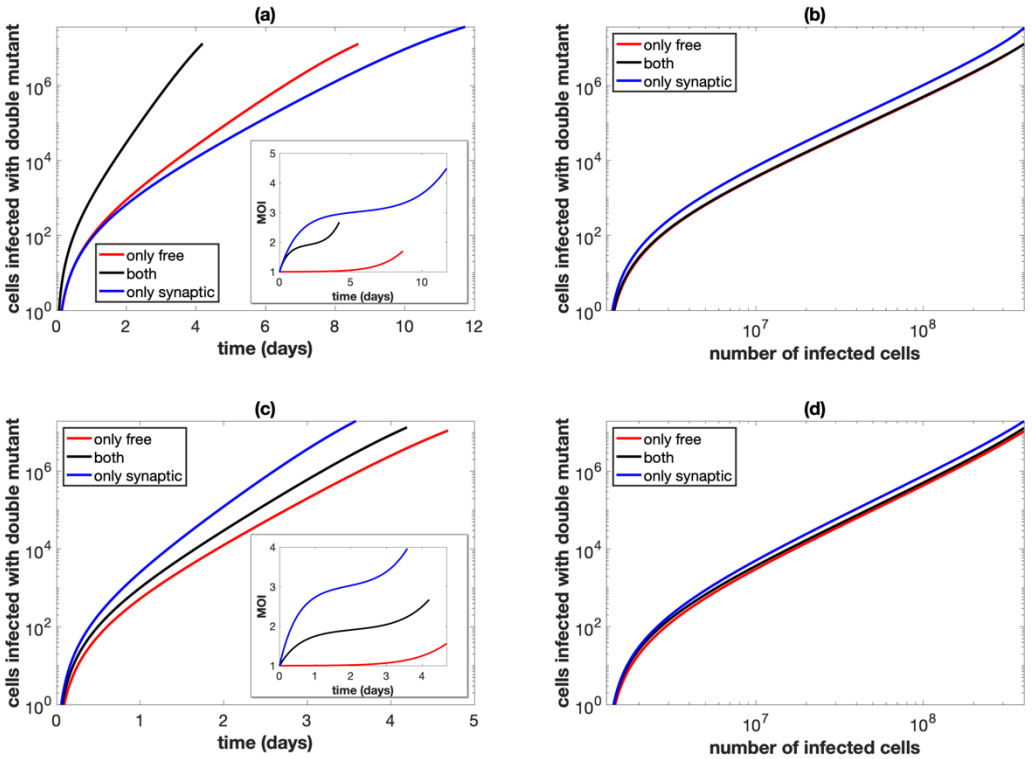

Figure 3: Evolutionary mutant dynamics. Simulations start with a small equal amount of cells singly infected with both single mutant strains. We assume we have 10^9 initial cells, and run the simulation until the number of infected cells reaches 40% of this initial amount, while also assuming that uninfected cells do not divide. Parameters are the best-fit parameters from static experiment B2, which are listed in Table 3 in the Supplementary Materials. The combination of both transmission pathways is represented by the black lines. For the only free virus transmission case (red lines), synaptic transmission is turned off. For the only synaptic transmission case (blue lines), free virus transmission and reinfection are turned off. For (a and b), we assume that the parameters are exactly as in the experiment. For (c and d) we assume that the overall growth rate is the same across the three cases. (a and c) Total number of cells infected with at least one active copy of double mutant virus plotted against time. The multiplicity of infection (MOI) is included in the inset. (b and d) Total number of cells infected with at least one active copy of double mutant virus plotted against the total number of cells infected with at least one active copy of virus.

give rise to two different kind of single-mutant viruses, and double mutant viruses can be generated either by recombination between the single mutants, or by additional point mutations in those single mutants (Figure 4). We start by considering the number of cells that contain two different single mutant viruses over time, since these cells form the basis for recombination. Despite the fact that the estimated rate of synaptic transmission is slower than the estimated rate of free virus transmission, the number of cells containing both single mutants rises sharply at low viral load in simulations that that take into account only synaptic transmission, compared to simulations that only take into account free virus transmission (Figure 4a). The reason is that (i) more reverse transcription events occur with synaptic transmission, thus generating more single mutant viruses (Figure 4a inset), and (ii) once the two different single mutant viruses have come together in the same cell, synaptic transmission enables their repeated co-transfer to target cells, explaining the sharp rise. As viral load grows to higher levels in the simulations, the number of cells containing both single mutants under free virus transmission overtakes those under synaptic transmission (Figure 4a) because at high viral loads, the rate of co-infection becomes relatively high even for free virus transmission, and the estimated rate of free virus transmission is faster than the rate of synaptic transmission. Looking at the number of double mutants (Figure 4(b and c)), we again observe that at a given infected cell population size, the number is highest for synaptic transmission only, the presence of both transmission pathways results in intermediate recombinant levels, and fewest recombinants are observed for free virus transmission only. The reason is the same as before, with the additional mechanism that point mutation accumulation is also accelerated under synaptic transmission due to

a higher number of reverse transcription events when multiple viruses are simultaneously transferred to the target cell. The same patterns are observed if we again adjust the overall virus growth rates such that they are identical regardless of transmission pathway and equal to the growth rate observed under static experimental conditions (Figure 4(d-f)).

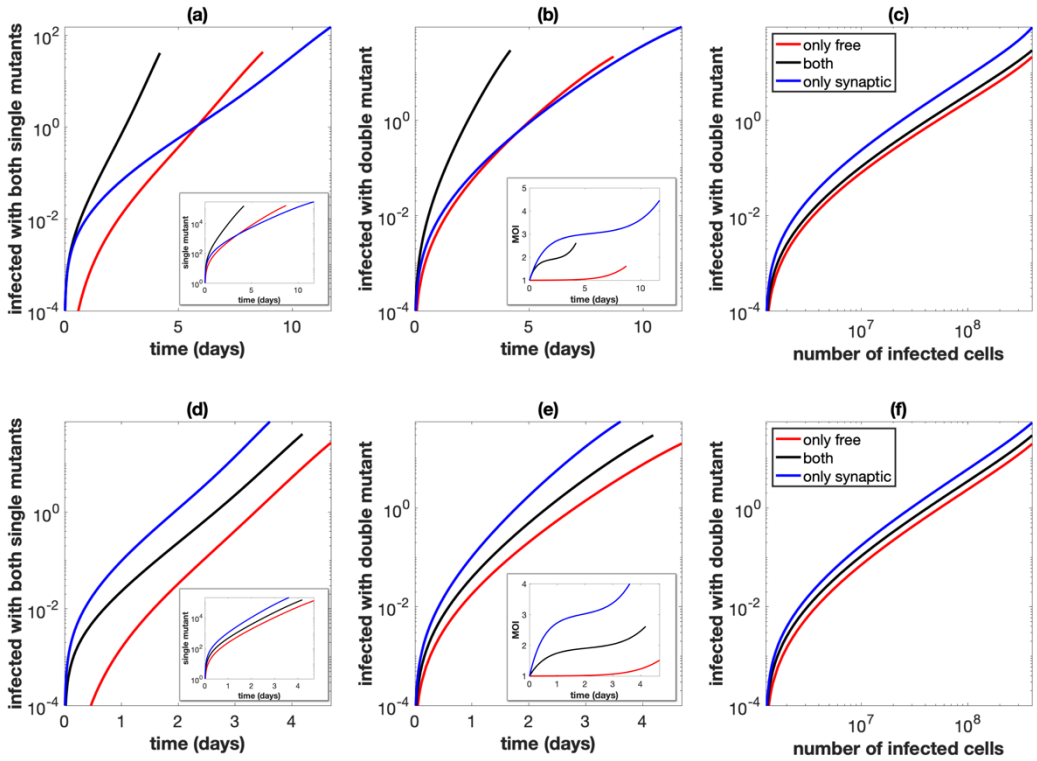

Figure 4: Evolutionary mutant dynamics. Same as in Fig. 3, but the simulations start with a small equal amount of cells singly infected with the wild type, and mutations are included. For (a-c), we assume that the parameters are exactly as in the experiment. For (d-f) we assume that the overall growth rate is the same across the three cases. (a and d) Total number of cells infected with at least one copy of either single mutant strain. The number of cells infected with at least one copy of one of the single mutants is included in the inset. (b and e) Total number of cells infected with at least one active copy of double mutant virus plotted against time. The multiplicity of infection (MOI) is included in the inset. (c and f) Total number of cells infected with at least one active copy of double mutant virus plotted against the total number of cells infected with at least one active copy of virus.

Again, it is important to note that both the emergence of single mutants, and the evolution of double mutants through recombination is accelerated by a higher average

infection multiplicity in cells, which is promoted by synaptic transmission (Figure 4(b and d inset)).

Discussion and Conclusion

In this study, we used mathematical models in combination with experimental data to determine the contribution of free virus transmission and direct cell-to-cell transmission to the evolution of recombinant viruses. This was possible through the use of experimental techniques to separate the two viral transmission pathways, and the use of fluorescent reporter viruses that allowed us to track recombinant evolution. Fitting of mathematical models to the experimental data allowed the estimation of important parameters that characterize the recombination process, and the models were further used to run evolutionary simulations to go beyond the experimental system and to quantify how the two transmission pathways influence the number of recombinants generated under a more complete set of evolutionary processes.

We found that direct cell-to-cell transmission through virological synapses strongly promotes the evolution of recombinants, due to the following mechanisms: (i) synaptic transmission increases the infection multiplicity of cells, which is the basis for recombinant generation; (ii) synaptic transmission promotes the repeated co-transmission of two different virus strains from cell to cell, which increases the chances to eventually generate a recombinant virus; (iii) synaptic transmission increases point mutation generation because the simultaneous transfer of multiple viruses to the target

cell increases the number of reverse transcription events, during which point mutations are mostly likely to occur. We estimated cell-to-cell transmission to result in the successful integration of about 3 viruses per synapse in the target cell, which gave rise to an average infection multiplicity of maximally eight at the highest virus levels in some of the experiments. Experiments have shown that tens to hundreds of virus particles can be simultaneously transmitted per synapse [17, 24], but it is likely that only a subset of these result in successful integration.

Interestingly, our analysis suggests that the addition of a free virus transmission component to a given rate of synaptic transmission reduces the number of recombinants. The reason is that in this case, a smaller fraction of the virus transmission events occurs through synapses during virus growth, which limits the evolutionary potential of the virus. Therefore, these results suggest that from the perspective of mutant evolution alone, the spread of the virus through the release of free viruses can be counter-productive. Free virus transmission, however, can provide other advantages, such as an acceleration of the overall rate of virus growth.

Our analysis also repeated some of our previous work [21] where we estimated the relative contribution of free virus and synaptic transmission to virus growth, using Jurkat cell lines. In this study, it was estimated that the two transmission pathways contributed more or less equally to virus spread, where the rate of free virus transmission was approximately 1.1 fold faster than the rate of synaptic transmission. In the present study, which used CEM-ss cells, we estimated the rate of free virus

transmission to be approximately 1.4 fold faster than the rate of synaptic transmission, which is a somewhat larger difference. The reason for this discrepancy could lie in the different cell types used, and in the fact that our current calculations took into account the possibility that entry of virus into uninfected cells can result in latent viruses that can be activated upon superinfection. It is further possible that in our current experiments, the formation of virological synapses between two cells is most likely among spatially clustered cells, as has been observed in vivo in humanized mice [18]. This can result in a slower increase in the number of infected cells.

Our study provides an important link between direct cell-to-cell transmission, heightened infection multiplicity, and an increased rate of recombinant (and single mutant) evolution. While this was established within the framework of in vitro experimentation, these notions are likely also relevant in vivo. Synaptic transmission has been clearly documented in vivo and infection multiplicities of cells in the tissue from HIV-infected patients have been shown to be between 3-4 or even higher on average [25]. Other studies reported the average infection multiplicities in the blood and tissue of HIV-infected patients to be closer to one [26, 27], although the restriction of the analysis to cells that express the CD4 receptor could have artificially lowered the estimate of infection multiplicities. The CD4 receptor becomes eventually down-regulated following the infection of the cell with the first virus. Ignoring such cells in the analysis could miss those cells with the highest infection multiplicities.

An interesting finding was that at the resolution of the data presented here, standard ordinary differential equations of virus dynamics failed to adequately describe several multiply infected cell subpopulations. We found that incorporating the assumption of limited mixing and the consequent re-infection of cells by their own offspring virus resulted in better model fits to the data. This might be important to keep in mind when modeling the multiple infection of cells in HIV infection.

Overall, our analysis points towards an important role of synaptic transmission for the rate of viral evolution, and emphasizes the importance of infection multiplicity for the outcome of viral evolutionary processes. Future studies should examine how these processes affect viral evolution under the assumption that mutants differ in fitness, and that the co-infection of cells with virus strains of different fitness can result in complementary and inhibitory interactions. The modeling framework and parameter estimates provided here form a basis for this future investigation.

References

1. Hirsch VM. Evolution of the fittest ends in tragedy. Nature medicine. 1999;5(5):488-9. PubMed PMID: 10229221.
2. Kimata JT, Kuller L, Anderson DB, Dailey P, Overbaugh J. Emerging cytopathic and antigenic simian immunodeficiency virus variants influence AIDS progression. Nature medicine. 1999;5(5):535-41. PubMed PMID: 10229230.
3. Bonhoeffer S, May RM, Shaw GM, Nowak MA. Virus dynamics and drug therapy. Proceedings of the National Academy of Sciences of the United States of America. 1997;94(13):6971-6.
4. Mansky LM, Temin HM. Lower in vivo mutation rate of human immunodeficiency virus type 1 than that predicted from the fidelity of purified reverse transcriptase. Journal of virology. 1995;69(8):5087-94. Epub 1995/08/01. PubMed PMID: 7541846; PubMed Central PMCID: PMC189326.
5. Wei XP, Ghosh SK, Taylor ME, Johnson VA, Emini EA, Deutsch P, et al. Viral Dynamics in Human-Immunodeficiency-Virus Type-1 Infection. Nature. 1995;373(6510):117-22.
6. Ho DD, Neumann AU, Perelson AS, Chen W, Leonard JM, Markowitz M. Rapid Turnover of Plasma Virions and Cd4 Lymphocytes in Hiv-1 Infection. Nature. 1995;373(6510):123-6.
7. Perelson AS, Neumann AU, Markowitz M, Leonard JM, Ho DD. Hiv-1 Dynamics in-Vivo - Virion Clearance Rate, Infected Cell Life- Span, and Viral Generation Time. Science. 1996;271(5255):1582-6.
8. Levy DN, Aldrovandi GM, Kutsch O, Shaw GM. Dynamics of HIV-1 recombination in its natural target cells. Proceedings of the National Academy of Sciences of the United States of America. 2004;101(12):4204-9. PubMed PMID: 15010526.
9. Moutouh L, Corbeil J, Richman DD. Recombination leads to the rapid emergence of HIV-1 dually resistant mutants under selective drug pressure. Proceedings of the National Academy of Sciences of the United States of America. 1996;93(12):6106-11. PubMed PMID: 8650227.
10. Bretscher MT, Althaus CL, Muller V, Bonhoeffer S. Recombination in HIV and the evolution of drug resistance: for better or for worse? Bioessays. 2004;26(2):180-8. PubMed PMID: 14745836.
11. Fraser C. HIV recombination: what is the impact on antiretroviral therapy? Journal of the Royal Society, Interface. 2005;2(5):489-503. PubMed PMID: 16849208.
12. Althaus CL, Bonhoeffer S. Stochastic interplay between mutation and recombination during the acquisition of drug resistance mutations in human immunodeficiency virus type 1. Journal of virology. 2005;79(21):13572-8. PubMed PMID: 16227277.
13. Carvajal-Rodriguez A, Crandall KA, Posada D. Recombination estimation under complex evolutionary models with the coalescent composite-likelihood method. Molecular biology and evolution. 2006;23(4):817-27. Epub 2006/02/03. doi: msj102 [pii] 10.1093/molbev/msj102. PubMed PMID: 16452117; PubMed Central PMCID: PMC1949848.
14. Kouyos RD, Fouchet D, Bonhoeffer S. Recombination and drug resistance in HIV: population dynamics and stochasticity. Epidemics. 2009;1(1):58-69.
15. Kreger J, Komarova NL, Wodarz D. Effect of synaptic cell-to-cell transmission and recombination on the evolution of double mutants in HIV. Journal of the Royal Society Interface. 2020;17(164):20190832.

16. Bonhoeffer S, Chappey C, Parkin NT, Whitcomb JM, Petropoulos CJ. Evidence for positive epistasis in HIV-1. Science. 2004;306(5701):1547-50. PubMed PMID: 15567861.
17. Hubner W, McNerney GP, Chen P, Dale BM, Gordon RE, Chuang FY, et al. Quantitative 3D video microscopy of HIV transfer across T cell virological synapses. Science. 2009;323(5922):1743-7. PubMed PMID: 19325119.
18. Law KM, Komarova NL, Yewdall AW, Lee RK, Herrera OL, Wodarz D, et al. In Vivo HIV-1 Cell-to-Cell Transmission Promotes Multicopy Micro-compartmentalized Infection. Cell reports. 2016;15(12):2771-83. doi: 10.1016/j.celrep.2016.05.059. PubMed PMID: 27292632.
19. Del Portillo A, Tripodi J, Najfeld V, Wodarz D, Levy DN, Chen BK. Multiploid inheritance of HIV-1 during cell-to-cell infection. Journal of virology. 2011;85(14):7169-76. Epub 2011/05/06. doi: JVI.00231-11 [pii]
10.1128/JVI.00231-11. PubMed PMID: 21543479; PubMed Central PMCID: PMC3126592.
20. Sourisseau M, Sol-Foulon N, Porrot F, Blanchet F, Schwartz O. Inefficient human immunodeficiency virus replication in mobile lymphocytes. Journal of virology. 2007;81(2):1000-12. Epub 2006/11/03. doi: JVI.01629-06 [pii]
10.1128/JVI.01629-06. PubMed PMID: 17079292; PubMed Central PMCID: PMC1797449.
21. Komarova NL, Anghelina D, Voznesensky I, Trinite B, Levy DN, Wodarz D. Relative contribution of free-virus and synaptic transmission to the spread of HIV-1 through target cell populations. Biol Lett. 2013;9(1):20121049. Epub 2012/12/28. doi: 10.1098/rsbl.2012.1049 rsbl.2012.1049 [pii]. PubMed PMID: 23269844; PubMed Central PMCID: PMC3565528.
22. Trinite B, Chan CN, Lee CS, Mahajan S, Luo Y, Muesing MA, et al. Suppression of Foxo1 activity and down-modulation of CD62L (L-selectin) in HIV-1 infected resting CD4 T cells. PLoS One. 2014;9(10):e110719. Epub 2014/10/21. doi: 10.1371/journal.pone.0110719. PubMed PMID: 25330112; PubMed Central PMCID: PMCPMC4199762.
23. Bregnard C, Pacini G, Danos O, Basmaciogullari S. Suboptimal provirus expression explains apparent nonrandom cell coinfection with HIV-1. Journal of virology. 2012;86(16):8810-20. doi: 10.1128/JVI.00831-12. PubMed PMID: 22696639; PubMed Central PMCID: PMC3421764.
24. Chen P, Hubner W, Spinelli MA, Chen BK. Predominant mode of human immunodeficiency virus transfer between T cells is mediated by sustained Env-dependent neutralization-resistant virological synapses. Journal of virology. 2007;81(22):12582-95. Epub 2007/08/31. doi: JVI.00381-07 [pii]
10.1128/JVI.00381-07. PubMed PMID: 17728240; PubMed Central PMCID: PMC2169007.
25. Jung A, Maier R, Vartanian J-P, Bocharov G, Jung V, Fischer U, et al. Multiply infected spleen cells in HIV patients. Nature. 2002;418(6894):144-.
26. Josefsson L, King MS, Makitalo B, Brannstrom J, Shao W, Maldarelli F, et al. Majority of CD4+ T cells from peripheral blood of HIV-1-infected individuals contain only one HIV DNA molecule. Proceedings of the National Academy of Sciences of the United States of America. 2011;108(27):11199-204. Epub 2011/06/22. doi: 1107729108 [pii]
10.1073/pnas.1107729108. PubMed PMID: 21690402; PubMed Central PMCID: PMC3131354.
27. Josefsson L, Palmer S, Faria NR, Lemey P, Casazza J, Ambrozak D, et al. Single cell analysis of lymph node tissue from HIV-1 infected patients reveals that the majority of CD4+ T-cells contain one HIV-1 DNA molecule. PLoS pathogens. 2013;9(6):e1003432. doi:

10.1371/journal.ppat.1003432. PubMed PMID: 23818847; PubMed Central PMCID: PMC3688524.